

## RESEARCH ARTICLE

# Individual-specific resting-state networks predict language dominance in drug-resistant epilepsy

Mervyn Jun Rui Lim<sup>1,2,3</sup>  | Shaoshi Zhang<sup>1</sup>  | Shreya Pande<sup>1</sup>  | Aihuiping Xue<sup>1</sup>  | Ru Kong<sup>1</sup>  | Kareem Zaghloul<sup>2</sup>  | Sara Inati<sup>2</sup>  | B. T. Thomas Yeo<sup>1</sup> 

<sup>1</sup>Computational Brain Imaging Group, Yong Loo Lin School of Medicine, National University of Singapore, Singapore, Singapore

<sup>2</sup>National Institute of Neurological Disorders and Stroke, National Institutes of Health, Bethesda, Maryland, USA

<sup>3</sup>Division of Neurosurgery, Department of Surgery, National University Hospital, Singapore, Singapore

## Correspondence

B. T. Thomas Yeo, Computational Brain Imaging Group, Yong Loo Lin School of Medicine, National University of Singapore, Tahir Foundation Building (MD1), 12 Science Drive 2, #13-05C, National University of Singapore, Singapore 117549.  
Email: [thomas.yeo@nus.edu.sg](mailto:thomas.yeo@nus.edu.sg)

Kareem Zaghloul and Sara Inati, National Institute of Neurological Disorders and Stroke, National Institutes of Health, 31 Center Drive, Bethesda, MD 20892, USA.  
Email: [kareem.zaghloul@nih.gov](mailto:kareem.zaghloul@nih.gov) and [sara.inati@nih.gov](mailto:sara.inati@nih.gov)

## Funding information

National Institutes of Health, Grant/Award Number: NIH-DIR ZIA NS009431-05; NUS Yong Loo Lin School of Medicine, Grant/Award Number: NUHSRO/2020/124/TMR/LOA; Singapore National Medical Research Council (NMRC), Grant/Award Number: OFLCG19May-0035; NMRC CTG-IIT, Grant/Award Number: CTGIIT23jan-0001; NMRC OF-IRG, Grant/Award Number: OFIRG24jan-0006; OFIRG24jul-0049; NMRC STaR, Grant/Award Number: STaR20nov-0003; Singapore Ministry of Health (MOH) Centre Grant, Grant/Award Number: CG21APR1009; United States National Institutes

## Abstract

**Objective:** This study was undertaken to reliably estimate individual-specific resting-state cortical networks and determine whether language network topography can predict task-based language dominance in drug-resistant epilepsy.

**Methods:** We utilized a multisession hierarchical Bayesian model (MS-HBM) trained on drug-resistant epilepsy patients to map high-quality individual-specific cortical networks in this population ( $n = 65$ ) with only 6–24 min of resting-state functional magnetic resonance imaging (fMRI). We compared the quality of networks to MS-HBM models trained on healthy participants from the human connectome project ( $n = 40$ ) and tested the generalizability of the model in an independent cohort of drug-resistant epilepsy participants ( $n = 26$ ). Resting-state language network topography was then used to predict task-based language dominance.

**Results:** Ninety-one participants with drug-resistant epilepsy (National Institutes of Health,  $n = 65$ ; University of Iowa,  $n = 26$ ) were included: 61 (67.0%) temporal lobe epilepsy, 29 (31.9%) extratemporal lobe epilepsy, and one (1.1%) undetermined seizure onset zone. The mean age was  $33.0 \pm 11.4$  years, and 50 (54.9%) were male. There were 40 healthy participants with a mean age of  $29.0 \pm 4.0$  years, and 16 (40.0%) were male. MS-HBM trained on drug-resistant epilepsy estimated individual-specific networks that more accurately capture cortical functional organization than group-average networks or MS-HBM trained on healthy participants. The trained MS-HBM model generalized to an independent cohort of drug-resistant epilepsy participants with concurrent intracranial electrical stimulation and fMRI. Critically, cortical evoked fMRI activity aligned more closely with individual-specific networks than with group-average networks. Furthermore,

Kareem Zaghloul, Sara Inati, and B. T. Thomas Yeo contributed equally to this work.

This is an open access article under the terms of the [Creative Commons Attribution-NonCommercial](https://creativecommons.org/licenses/by-nc/4.0/) License, which permits use, distribution and reproduction in any medium, provided the original work is properly cited and is not used for commercial purposes.

© 2026 The Author(s). *Epilepsia* published by Wiley Periodicals LLC on behalf of International League Against Epilepsy.

of Health, Grant/Award Number: R01MH133334&2R01MH120080; Singapore National Research Foundation (NRF) Investigatorship, Grant/Award Number: NRF110-2024-0014

individual-specific language network topography significantly predicted task-based language dominance, achieving high accuracy for left (area under the curve [AUC] = .82), bilateral (AUC = .72), and right (AUC = .83) dominance.

**Significance:** These results demonstrate that MS-HBM captures functionally meaningful network reorganization in drug-resistant epilepsy and enables accurate, individual-level prediction of language lateralization, with direct implications for presurgical functional mapping.

#### KEYWORDS

functional magnetic resonance imaging, language lateralization, multisession hierarchical Bayesian model, precision functional mapping

## 1 | INTRODUCTION

Identifying the hemisphere of language dominance is a crucial step in planning surgery for epilepsy, as it has direct implications for preoperative counseling and postsurgical language outcomes.<sup>1</sup> Current clinical guidelines recommend task-based functional magnetic resonance imaging (fMRI) as a noninvasive alternative to reduce complications from the intracarotid amobarbital test.<sup>2–4</sup> In this context, task-based language dominance refers to the hemispheric asymmetry of language processing, assessed by comparing the extent of language-related task-fMRI activation between the left and right hemispheres during language tasks. However, task-based fMRI is highly dependent on patient compliance and task design.<sup>5,6</sup> Resting-state fMRI avoids these limitations by removing the need for patient participation and can map multiple brain functions using a single scan.<sup>7</sup>

However, prior studies using resting-state fMRI to predict task-based language dominance in drug-resistant epilepsy have reported only modest prediction accuracy,<sup>8–11</sup> possibly because previous methods were unable to fully account for interindividual variability in language network topography. Furthermore, although numerous studies have reported alterations in resting-state functional connectivity in drug-resistant epilepsy,<sup>12–15</sup> far less is known about the organization and behavioral relevance of individual-specific cortical networks in this population. Thus, we aimed to characterize individual-specific cortical networks and investigate the clinical utility of the language networks for improving prediction of language dominance in participants with drug-resistant epilepsy using a precision functional mapping approach.

Precision functional mapping is a technique used to delineate functional brain organization using resting-state fMRI at the individual level rather than relying on population-averaged atlases.<sup>16–19</sup> This approach is

#### Key points

- Existing resting-state fMRI methods have limited ability to predict language dominance for epilepsy surgery.
- Precision functional mapping techniques allow reliable estimation of interindividual variability in large-scale resting-state networks.
- MS-HBM can map high-quality individual-specific cortical networks in drug-resistant epilepsy using only 6–24 min of data.
- Individual-specific language network topography predicted task-based language dominance well in individual patients.

motivated by interindividual variability in large-scale functional networks<sup>17,18</sup> as well as systemic differences between healthy and pathological brains.<sup>20,21</sup> Thus, mapping the individual's functional networks in neurological and psychiatric disease<sup>22</sup> holds promise for prognostication,<sup>21</sup> network-guided neuromodulation,<sup>23</sup> and neurosurgical practice.<sup>24</sup>

A major barrier to clinical translation, however, has been the long scan duration—at least 1 h—traditionally required for precision functional mapping.<sup>20,21,25</sup> We previously developed a multisession hierarchical Bayesian model (MS-HBM) that overcomes this limitation by enabling reliable estimation of individual-specific networks from limited data; MS-HBM networks obtained using only 10 min of data were comparable to other approaches requiring 50 min of data.<sup>26</sup> Individual-specific differences in MS-HBM network topography have been shown to predict interindividual variation in cognition and mental health<sup>26</sup> and aligned with individual-level task-evoked activity.<sup>16</sup> By substantially reducing scan time requirements, this approach might enable precision functional mapping to

become feasible in routine clinical settings, where patients might not be able to tolerate long scans.

In this study, we demonstrate that MS-HBM trained on drug-resistant epilepsy patients can be used to map high-quality individual-specific cortical networks in this population using only 6–24 min of resting-state fMRI (which was the range of scan durations in both drug-resistant epilepsy cohorts analyzed). The resulting individual-specific cortical networks conformed better to new resting-state fMRI data from the same participants than both group-average networks and MS-HBM trained on healthy individuals. Furthermore, in an independent drug-resistant epilepsy cohort with concurrent intracranial electrical stimulation and fMRI,<sup>27</sup> cortical evoked activity aligned better with individual-specific networks than with group-average networks. Finally, we showed that individual-specific language network topography predicted task-based language dominance well in individual patients. Together, these findings demonstrate that MS-HBM can capture individual-specific network organization in epilepsy and reliably predict language lateralization in individuals.

## 2 | MATERIALS AND METHODS

### 2.1 | Participants and datasets

In this study, we included one open-source dataset of healthy participants and two independent datasets of participants with drug-resistant epilepsy undergoing presurgical evaluation. Human Connectome Project (HCP) participants had a mean age of  $29.0 \pm 4.0$  years, 16 (40.0%) were male, and 12 (30.0%) self-reported as non-White and/or Hispanic. National Institutes of Health (NIH) epilepsy participants had a mean age of  $31.9 \pm 11.2$  years, and 33 (50.8%) were male. Of these, 42 (64.6%) had temporal lobe epilepsy and 23 (35.4%) had extratemporal lobe epilepsy (Table S1). Electrical stimulation fMRI (esfmri) participants had a mean age of  $35.8 \pm 11.5$  years, and 17 (65.4%) were male. Of these, 19 (73.1%) had temporal lobe epilepsy, six (23.1%) had extratemporal lobe epilepsy, and one (3.8%) had undetermined seizure onset zone (Table S2).

All datasets included structural and resting-state fMRI scans. In the esfmri dataset, postoperative fMRI was acquired with concurrent intracranial electrical stimulation delivered through stereoecephalographic electrodes and interleaved with echo planar imaging volume acquisition.<sup>27</sup> Alternating blocks of approximately 30 s of no stimulation or stimulation were delivered during the fMRI scan. No cognitive task was given to the participant, and no behavioral effects were evoked during the stimulation period. Preprocessing of imaging data followed the

surface-based pipeline of Yeo et al.<sup>28,29</sup> Further details regarding the demographics, data collection, and preprocessing are provided in the Supplementary Methods. After preprocessing, there were 40 HCP participants with four runs each. Of the 48 NIH participants with two or more runs, 34 (70.8%) participants were used for the training set, and 14 (29.2%) participants were used for the test set. For the esfmri dataset, there were 11 participants that had at least two valid preoperative runs and 17 participants that had at least two valid postoperative runs (Figure 1A).

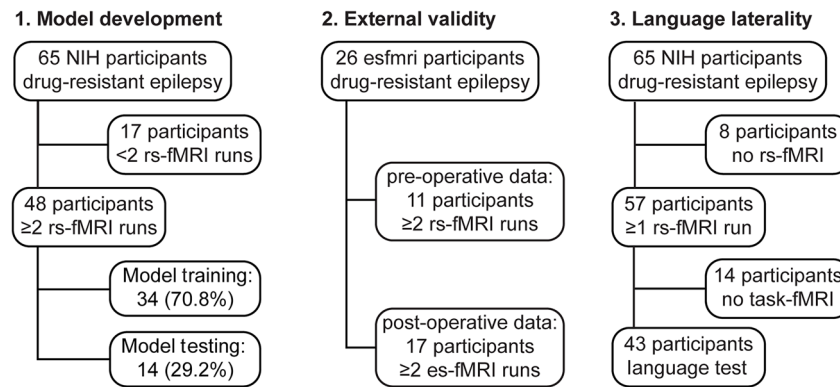
### 2.2 | Derivation of group-average networks and training of MS-HBM for estimating individual-specific networks

Our approach has been described previously.<sup>26,29</sup> At each cortical region (81 924 vertices), Pearson correlation between the fMRI time series and 1175 regions of interests were binarized by keeping the top 10% of correlations. The connectivity profiles were then clustered using a mixture of von Mises–Fisher distributions to derive the group-average 15 networks.<sup>29,30</sup> The 15-network solution used in this study follows prior work and can be grouped into nine canonical functional systems, including visual, somatomotor, auditory, limbic, control, dorsal attention, salience/ventral attention, language, and default networks.<sup>16,29</sup> In addition to computing group-average networks for the 40 HCP participants and 34 NIH participants, we also compared our results to group-average networks derived from an independent dataset of 15 intensively sampled healthy participants.<sup>16</sup> Next, we trained MS-HBM models on either the 40 HCP participants (using the HCP group average or Du group average) or 34 NIH participants to estimate model parameters. Further details on the training of MS-HBM may be found in the Supplementary Methods. Individual-specific networks were visually confirmed using model-free seed-based functional connectivity. Intersubject similarity in network topography across the 15 networks was quantified using the Dice similarity coefficient across all 57 NIH participants with at least one valid run.

### 2.3 | Validation and generalization of MS-HBM trained on drug-resistant epilepsy

To evaluate the quality of individual-specific networks estimated from MS-HBM trained on drug-resistant epilepsy or healthy participants, we computed two previously established metrics<sup>17,18,26,31,32</sup>: the weighted resting-state connective homogeneity and weighted task (electrical

## (A) Overview of analysis and population flowcharts



## (B) Model training for estimating individual-specific networks

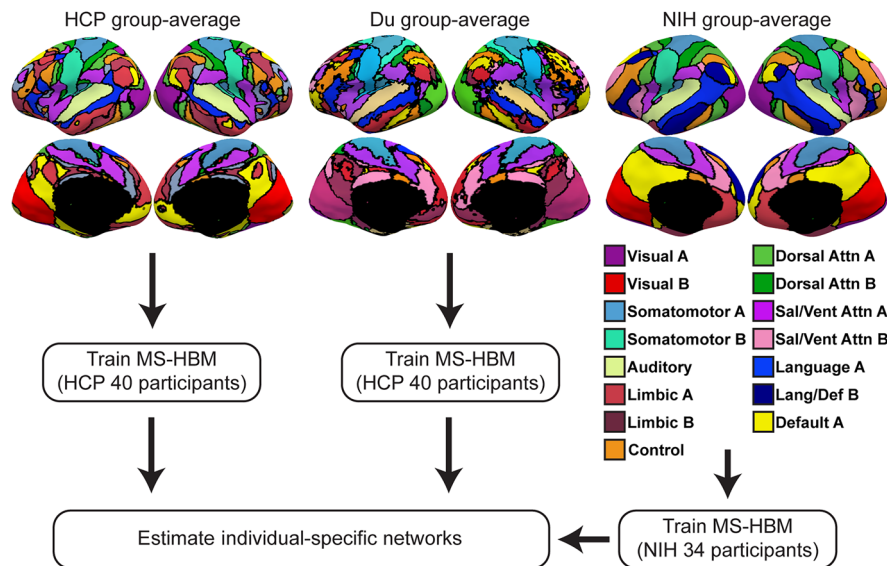


**FIGURE 1** Study overview and population flowchart. (A) We developed a multisession hierarchical Bayesian model (MS-HBM) model for estimating individual-specific networks in drug-resistant epilepsy, validated and tested the model in an independent dataset, and showed that the topography of individual-specific language networks was able to predict task-based language dominance. (B) Group-average networks from healthy participants of the Human Connectome Project (HCP) dataset, the Du atlas, or drug-resistant epilepsy participants from the National Institutes of Health (NIH) dataset were used to train different MS-HBM models. Fifteen network labels were shown for NIH group-average networks. Networks in drug-resistant epilepsy appeared more focal compared to healthy participants. Attn, attention; esfmri, electrical stimulation functional magnetic resonance imaging; Lang, language; Def, default; rs-fMRI, resting-state functional magnetic resonance imaging; Sal, salience; Vent, ventral.

stimulation) functional inhomogeneity. These metrics encode the principle that if an individual-specific network captured the system-level organization of the individual's cortex, each network should exhibit homogeneous connectivity and function.

We first evaluated the resting-state homogeneity of each network on the NIH test set of 14 participants that were not used for training MS-HBM. The generalizability of the MS-HBM model was then tested using preoperative (11 participants) and postoperative (17 participants) esfmri data, as well as task inhomogeneity during electrical stimulation in the postoperative data. For estimating individual-specific networks in the

postoperative data, we used only blocks with no stimulation after discarding the first four frames of each block to remove residual effects of the hemodynamic response from the previous block.<sup>33</sup>

To ensure that runs used for estimating individual-specific networks were independent from runs used for computing evaluation metrics, we used a leave-one-run-out cross-validation method. For each participant with  $n$  valid runs, individual-specific networks were estimated using  $n - 1$  runs, and evaluation metrics were computed on the left-out run. This was repeated for all runs, and an average result was obtained for each participant. Statistical tests were performed using two-tailed paired

*t*-tests between each pair of networks (*df*=number of participants – 1). Statistical significance was taken to be  $q < .05$  after false discovery rate correction.

The average resting-state homogeneity and task inhomogeneity were compared across six networks: (1) HCP group-average networks, (2) individual-specific networks estimated using HCP MS-HBM, (3) Du group-average networks, (4) individual-specific networks estimated using Du MS-HBM, (5) NIH group-average networks, and (6) individual-specific networks estimated using NIH MS-HBM. Resting-state homogeneity was computed by averaging the Pearson correlations between each vertex's time course and the average time course of its network. The correlations were then averaged across all 15 networks while accounting for network size.<sup>26,31,32</sup> Thus, resting-state homogeneity measures the similarity of fMRI time series among vertices within the same network, with higher values indicating that network assignments reflect coherent functional organization.

Task inhomogeneity was computed as the average SD of cortical activation *z*-scores within each network from unthresholded generalized linear models of intracranial electrical stimulation.<sup>34</sup> The SD was then averaged across all 15 networks while accounting for network size.<sup>26,31,32</sup> Thus, task inhomogeneity measures the variability of evoked activation within each network, with lower values indicating that network boundaries more accurately separate functionally distinct regions. Further details on the computation of the generalized linear models are provided in the Supplementary Methods. To visualize the effects of intracranial electrical stimulation on cortical networks, group-average network boundaries and individual-specific network boundaries were overlaid on the electrical stimulation *z*-score activation maps. We hypothesized that electrical stimulation-evoked activity would align more closely to individual-specific network boundaries than group-average network boundaries.

## 2.4 | Predicting language dominance using individual-specific network topography

All patients underwent language task fMRI using an auditory description decision task as described previously.<sup>6,11</sup> Task-based language dominance was determined by a trained epileptologist (S.I.) through visual inspection of activation maps in the frontal and temporal regions at three thresholds ( $p < .01$ ,  $p < .001$ , top 10% of activations) and confirmed at a multidisciplinary epilepsy conference. Task-based language dominance refers to the dominant hemisphere for language, assessed

by comparing the extent of cortical activation between the left and right hemispheres during the auditory description decision task. There were a total of 43 NIH participants with valid task language dominance and at least one valid resting-state fMRI run.

In several participants with drug-resistant epilepsy, regions typically associated with the language network exhibited connectivity patterns characteristic of the default mode network, suggesting network reorganization. To capture this variability, we computed a resting-state laterality index (LI) based on the network topography of both the Language A and Language/Default B networks:

$$\text{Resting - state LI} = \frac{LH - RH}{LH + RH} \quad (1)$$

where LH and RH represent the number of vertices in the left and right hemispheres, respectively, assigned to the individual-specific Language A and Language/Default B networks. Unlike task-based fMRI, resting-state fMRI does not provide stimulus-evoked activation magnitudes. Thus, the laterality index was computed based on the number of vertices assigned to the language networks in each hemisphere, reflecting the spatial distribution of language network topography. Resting-state LI values for participants with left, bilateral, or right task-based language dominance were compared using one-way analysis of variance, with  $p < .05$  considered statistically significant. Finally, receiver operating curves and area under the curve statistics were computed to evaluate the predictive power of resting-state LI for each language dominance group.

## 3 | RESULTS

### 3.1 | Participants and datasets

We analyzed 131 participants, including 40 healthy participants from the HCP, 65 participants with drug-resistant epilepsy from the NIH epilepsy center, and 26 participants with drug-resistant epilepsy from the University of Iowa (esfmri dataset). HCP participants had a mean age of  $29.0 \pm 4.0$  years, and 16 (40.0%) were male. NIH participants had a mean age of  $31.9 \pm 11.2$  years, and 33 (50.8%) were male. Forty-two (64.6%) participants had temporal lobe epilepsy, and 23 (35.4%) had extratemporal lobe epilepsy (Table S1). esfmri participants<sup>27</sup> had a mean age of  $35.8 \pm 11.5$  years, and 17 (65.4%) were male. Nineteen (73.1%) participants had temporal lobe epilepsy, six (23.1%) had extratemporal lobe epilepsy, and one (3.8%) had undetermined seizure onset zone (Table S2). Further details regarding the data collection and preprocessing are provided in Materials and Methods.

### 3.2 | Model training and testing

We analyzed 40 HCP and 48 NIH participants who had two or more resting-state fMRI runs to train and test MS-HBM. Participants used for training MS-HBM models were kept separate from participants used for testing the quality of individual networks estimated by MS-HBM. Of the 48 NIH participants, 34 (70.8%) were used for the training dataset, and 14 (29.2%) were used for testing dataset (Figure 1A). To train MS-HBM models, we first estimated group-average networks of the 40 HCP participants and 34 NIH participants.<sup>29</sup> We also compared our results to group-average networks derived from an independent dataset of 15 intensively-sampled healthy participants from Du et al.<sup>16</sup>

Group-average networks in drug-resistant epilepsy were categorized into nine canonical groups (visual, somatomotor, auditory, limbic, control, dorsal attention, salience/ventral attention, language, and default), which were broadly consistent with prior literature.<sup>16,26,29,35</sup> Group-average networks in healthy participants were more spatially distributed than those in drug-resistant epilepsy (Figure 1B). For example, association networks such as the control network were subdivided into three networks in HCP data,<sup>26</sup> but were represented by a single, less distributed network in drug-resistant epilepsy. Instead, two spatially focal limbic networks emerged in orbitofrontal and parahippocampal regions. These differences were not explained by motion, as the average relative root mean square framewise displacement was  $.059 \pm .023$  versus  $.076 \pm .015$  and the average voxelwise differentiated signal variance was  $23.0 \pm 4.6$  versus  $58.4 \pm 6.8$  for the NIH dataset compared to the HCP dataset, respectively.

To better understand differences in group-average networks between drug-resistant epilepsy and healthy participants, we computed the correlation of the group-average functional connectivity between the two groups (Figure 1). In primary sensory and motor regions, there was high similarity (yellow) between the two groups. However, regions of lower similarity (red) were apparent along network boundaries and in higher order association cortex. These differences were further illustrated using seed-based functional connectivity to show that despite using identical seeds, there were clear visual differences between the HCP and NIH group-average functional connectivity (Figure S2).

Next, we computed MS-HBM parameters using data from (1) the 40 HCP participants and the HCP group average (HCP MS-HBM), (2) the 40 HCP participants and the Du group average (Du MS-HBM), or (3) the 34 NIH participants and the NIH group average (NIH MS-HBM). After training MS-HBM, each model was then used to estimate individual-specific networks in the NIH participants with

drug-resistant epilepsy. Using NIH MS-HBM, individual-specific networks captured interindividual variability while preserving canonical topographical features of healthy participants. Notably, some participants showed altered language network organization; inferior frontal language regions exhibited stronger connectivity with middle temporal and temporopolar areas typically associated with the default mode network in healthy individuals (Figure 2A,B). These differences in language network connectivity were visually confirmed using identical seeds placed in the inferior frontal and lateral temporal regions across participants (Figure 2C).

Quantitatively, intersubject variability was highest in the association networks such as the salience/ventral attention, dorsal attention, control, and language networks (Dice similarity coefficient = .35–.50), as compared to the somatomotor and visual networks (Dice similarity coefficient = .66–.71; Figure 2D). Comparing intersubject variability of the NIH drug-resistant epilepsy cohort to the intersubject variability of the HCP test set of 596 subjects from Kong et al.<sup>26</sup> (Figure S3B), we note that both groups show a similar spatial pattern of higher similarity in primary sensory/motor cortex and lower similarity in association cortex. However, the epilepsy cohort showed notably lower intersubject similarity in association regions (Dice similarity coefficient = .35–.50) compared to healthy controls (Dice similarity coefficient = .51–.61). This increased idiosyncrasy in the epilepsy group further motivates the use of individual-specific networks, as group-average networks would fail to capture the individual variability in drug-resistant epilepsy.

Finally, in the held-out set of 14 NIH participants, we compared the quality of individual-specific networks estimated from the three MS-HBM models and group-average networks from the HCP data, Du atlas, or NIH data using an established metric, resting-state connectional homogeneity.<sup>17,18,26,31,32</sup> To ensure that runs used for estimating individual-specific networks were independent from runs used for computing evaluation metrics, we used a leave-one-run-out cross-validation method. For each participant with  $n$  valid runs, individual-specific networks were estimated using  $n - 1$  runs, and evaluation metrics were computed on the left-out run. This was repeated for all runs, and an average result was obtained for each participant. We observed that individual-specific networks estimated using NIH MS-HBM performed significantly better than all group-average networks (HCP group:  $p < .001$ , Du group:  $p < .001$ , NIH group:  $p = .003$ ) and MS-HBM trained on healthy participants (HCP MS-HBM:  $p < .001$ , Du MS-HBM:  $p < .001$ ), even after correcting for multiple comparisons (Figure 3A). Notably, these results were consistent when the analysis was repeated specifically for the language networks (Figure S4A), which showed high

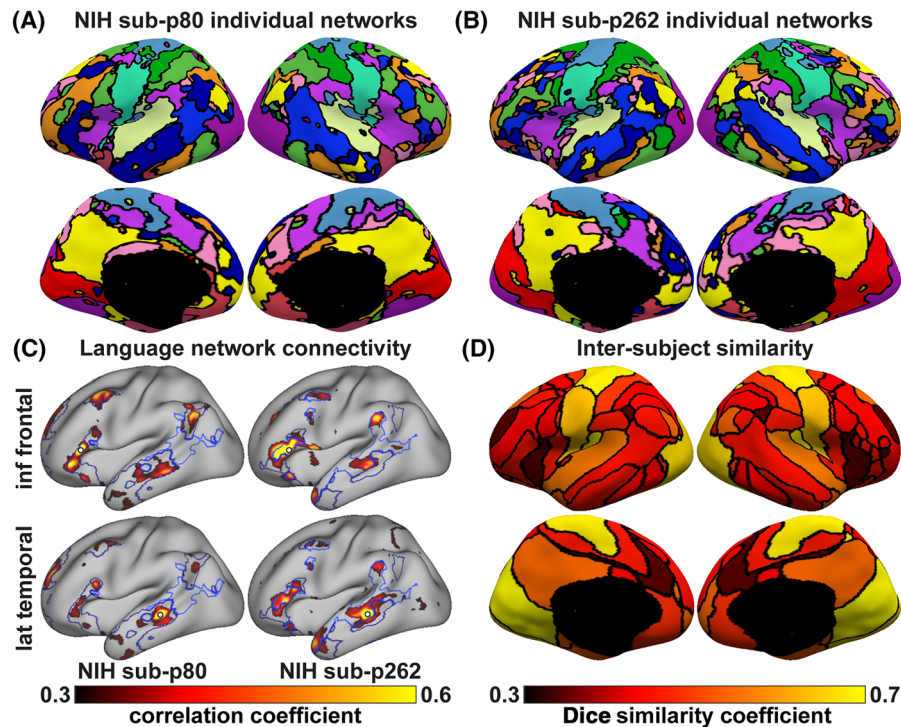


**FIGURE 2** Individual-specific resting-state cortical networks in drug-resistant epilepsy. (A, B) Individual-specific networks of two representative National Institutes of Health (NIH) participants estimated using the NIH multisession hierarchical Bayesian model. (C) Language network boundaries of both participants showing functional connectivity from identical seeds placed in the inferior (inf) frontal and lateral (lat) temporal region to different language networks in the two subjects. (D) Dice similarity coefficient for the 15 networks across all 57 NIH participants. Higher Dice coefficients (yellow) indicate greater intersubject topographic similarity, whereas lower Dice coefficients (dark red) indicate higher variability. Intersubject variability in drug-resistant epilepsy is higher in association than sensory networks. sub-p80, sub-p262 denotes subject number 80 and subject number 262.

interindividual variability in the drug-resistant epilepsy cohort.

### 3.3 | Validation in an independent dataset

MS-HBM trained on healthy participants might perform worse than NIH MS-HBM because of site and scanner differences. Therefore, we tested whether NIH MS-HBM was generalizable to an independent dataset of drug-resistant epilepsy.<sup>27</sup> In the esfmri dataset, there were 11 participants who had at least two preoperative runs and 17 participants who had at least two postoperative runs (Figure 1A). We observed that individual-specific networks estimated using NIH MS-HBM performed significantly better in resting-state homogeneity than all group-average networks and MS-HBM trained on healthy participants ( $p < .001$  for all comparisons using either the preoperative or postoperative data), even after correcting for multiple comparisons (Figure 3B,C).

In the esfmri dataset, postoperative fMRI was acquired with concurrent intracranial electrical stimulation

delivered through stereoencephalographic electrodes that was interleaved with echo planar imaging volume acquisition using alternating blocks of 30 s of stimulation or no stimulation.<sup>27</sup> Thus, we used a second established metric, task (electrical stimulation) inhomogeneity, to compare the quality of the individual-specific or group-average networks. Cortical evoked activity during electrical stimulation was computed using generalized linear models,<sup>34</sup> and electrical stimulation inhomogeneity was computed using the average SD of cortical activation  $z$ -scores within each network while accounting for network size.<sup>26,31,32</sup> A higher SD indicated higher task inhomogeneity.

We observed that individual-specific networks estimated using NIH MS-HBM performed significantly better than all group-average networks for electrical stimulation inhomogeneity (HCP group:  $p < .001$ , Du group:  $p < .001$ , NIH group:  $p = .002$ ), even after correcting for multiple comparisons (Figure 4A). During concurrent intracranial electrical stimulation and fMRI scans, cortical evoked activity aligned better with individual-specific network boundaries than group-average network boundaries (Figure 4B). These results were consistent when the analyses were repeated specifically for the language networks

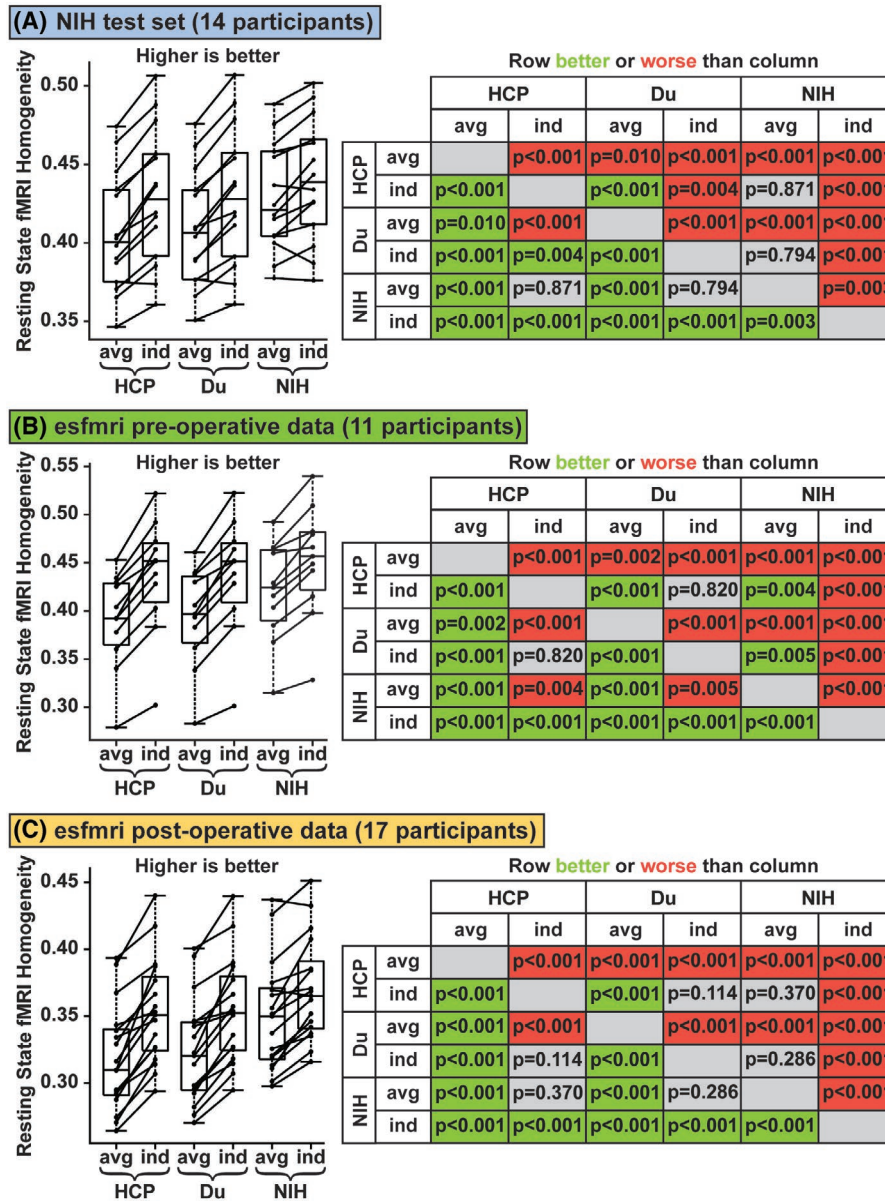


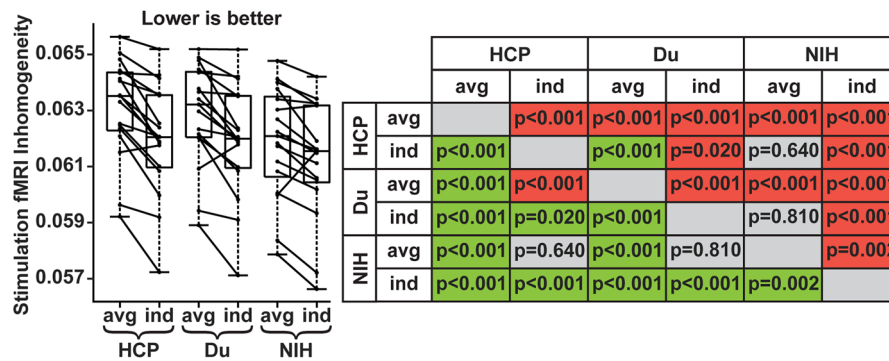
**FIGURE 3** Resting-state homogeneity of group-average (avg) and individual (ind)-specific networks. Individual-specific networks estimated using the National Institutes of Health (NIH) multisession hierarchical Bayesian model (MS-HBM) outperformed group-average networks or MS-HBM trained on healthy participants. Results were consistent across the (A) NIH test set, (B) electrical stimulation functional magnetic resonance imaging (esfmri) preoperative data, and (C) esfmri postoperative data. Six different networks were evaluated: (1) group-average and (2) individual-specific networks estimated from the Human Connectome Project (HCP) data; (3) group-average and (4) individual-specific networks estimated from the Du atlas; and (5) group-average and (6) individual-specific networks estimated from the NIH data. Left: boxplots of median resting-state homogeneity. Right: *t*-test *p*-values comparing pairs of approaches. Green indicates that the approach on the row performed significantly better than the column, red indicates worse, and gray indicates nonsignificant differences, after correcting for multiple comparisons using a false discovery rate of  $q < .05$ . fMRI, functional magnetic resonance imaging.

(Figure S4B–D). Taken together, these results suggest that NIH MS-HBM estimated high-quality, generalizable individual-specific networks that captured the functional organization of the cortex better than group-average networks or MS-HBM trained using healthy participants.

Finally, we evaluated model performance as a function of training dataset size by training MS-HBM using subsets of 5, 10, 15, 20, 25, and 30 participants, and comparing

performance to the full training set of 34 participants (Figure S5). Across all evaluation metrics, performance improved with increasing training sample size up to 20–25 participants. Beyond 20 participants, performance improvements became progressively smaller and statistically nonsignificant, suggesting that relatively modest sample sizes were sufficient to achieve near-optimal performance with MS-HBM.

## (A) esfmri post-operative data (17 participants)



## (B) sub-339 run-01 electrical stimulation evoked activity

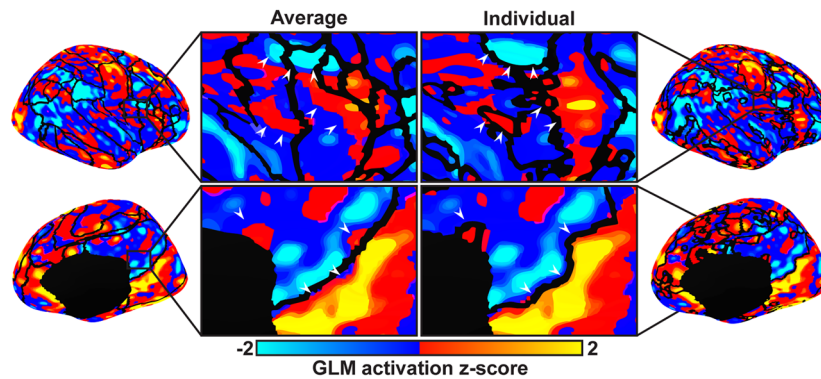


**FIGURE 4** Electrical stimulation inhomogeneity and evoked cortical activation map. Individual (ind)-specific networks estimated using the National Institutes of Health (NIH) multisession hierarchical Bayesian model performed the best in electrical stimulation inhomogeneity, and network boundaries aligned better to electrical stimulation-evoked activity compared to group-average (avg) networks. (A) Left shows boxplots of median electrical stimulation inhomogeneity across the six networks: (1) group-average and (2) individual-specific networks estimated from the Human Connectome Project (HCP) data; (3) group-average and (4) individual-specific networks estimated from the Du atlas; and (5) group-average and (6) individual-specific networks estimated from the NIH data. Right: *t*-test *p*-values comparing pairs of approaches. Green indicates that the approach on the row performed significantly better than the column, red indicates worse, and gray indicates nonsignificant differences, after correcting for multiple comparisons using a false discovery rate of  $q < .05$ . (B) Generalized linear model (GLM) of electrical stimulation during functional magnetic resonance imaging (fMRI) showing *z*-score normalized beta-coefficients overlaid with the NIH group-average network boundaries on the left and the participant's individual-specific network boundaries on the right. White arrowheads show evoked activity that aligned better with individual-specific networks than group-average networks. esfmri, electrical stimulation fMRI.

### 3.4 | Prediction of task-based language dominance

Having shown that individual-specific networks more accurately captured the functional organization of the cortex, we next focused specifically on the language networks, given their critical role in presurgical planning for drug-resistant epilepsy. We hypothesized that individual-specific language network topography would be particularly informative for predicting language dominance and tested whether the resting-state LI was able to predict task-based language dominance. Resting-state LI differed significantly across left (mean  $LI = .165 \pm .106$ ), bilateral (mean  $LI = .056 \pm .074$ ), and right (mean  $LI = .023 \pm .055$ ) task-based language dominance ( $p = .002$ ). Receiver operating curve analyses

showed area under the curve statistics of .82 for left, .72 for bilateral, and .83 for right language dominance versus other participants (Figure 5 and Figure S6). Conversely, individual-specific networks estimated using MS-HBM trained on healthy participants were not able to differentiate between task-based language dominance (HCP MS-HBM:  $p = .150$ , Du MS-HBM:  $p = .303$ ).

## 4 | DISCUSSION

In this study, we demonstrate that MS-HBM can reliably estimate individual-specific networks in drug-resistant epilepsy using only 6–24 min of resting-state fMRI data, despite altered structural and functional connectivity. Moreover, NIH MS-HBM captured the organization of

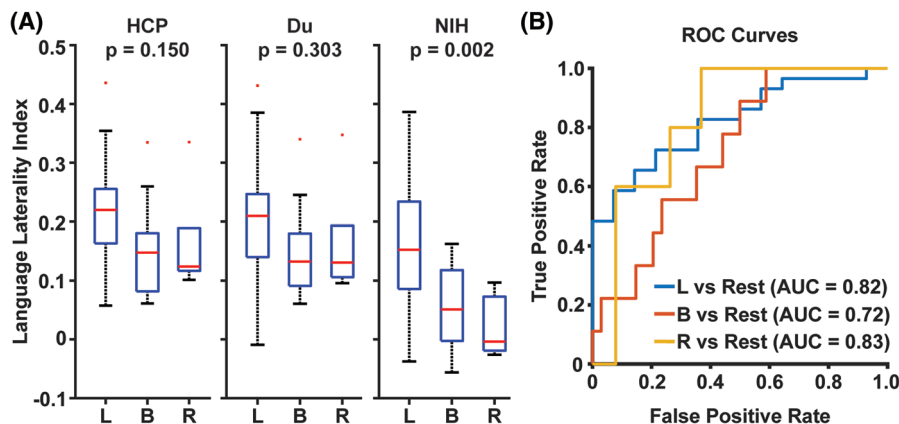


**FIGURE 5** Individual-specific language network topography predicts task-based language dominance. (A) Boxplots of language laterality index for participants with left (L), bilateral (B), or right (R) language dominance derived from task functional magnetic resonance imaging, comparing individual-specific networks estimated from Human Connectome Project (HCP) multisession hierarchical Bayesian model (MS-HBM), Du MS-HBM, or National Institutes of Health (NIH) MS-HBM. (B) Receiver operating characteristic (ROC) curves and area under the curve (AUC) statistics for predicting language dominance using individual-specific networks estimated by NIH MS-HBM.

an individuals' cerebral cortex better than group-average networks and generalized to an external dataset of drug-resistant epilepsy despite site, scanner, and preprocessing differences. Finally, we showed that individual-specific language network topography predicts task-based language dominance well in individual patients with drug-resistant epilepsy.

Existing evidence indicates that focal epilepsy is associated with reduced network integration and increased segregation, changes that may underlie the cognitive and behavioral comorbidities commonly observed in epilepsy.<sup>36,37</sup> Although approaches such as coordinate-based network mapping have successfully delineated an idiopathic generalized epilepsy network,<sup>13</sup> they are limited in their ability to characterize epilepsy-related reorganization of intrinsic resting-state networks at the individual level. As a result, cortical network organization in drug-resistant epilepsy, particularly alterations to canonical resting-state networks, remains incompletely characterized.<sup>38</sup> Consistent with these limitations, prior resting-state fMRI approaches were unable to reliably estimate individual-specific cortical organization of the language networks and predict task-based language dominance in drug-resistant epilepsy.<sup>8–11</sup> This gap likely reflects both the limited availability of high-quality resting-state fMRI data in clinical populations and the substantial heterogeneity of pathology in drug-resistant epilepsy.<sup>39</sup>

By leveraging MS-HBM, we begin to reveal the functional organization of focal drug-resistant epilepsy, with a particular focus on language networks. Although cortical networks in drug-resistant epilepsy broadly resemble canonical resting-state networks observed in healthy participants, their spatial topography is more focal,<sup>40,41</sup> and

individual-level variations emerge that are not typically seen in healthy brains. These differences cannot be explained by motion and likely arise from both group-level differences in functional connectivity and increased inter-individual variability in drug-resistant epilepsy. Notably, inferior frontal language regions in some participants exhibit stronger connectivity with areas typically associated with the default mode network in healthy individuals, potentially reflecting the long-term effects of chronic epileptogenic activity on functional connectivity.<sup>42,43</sup> By capturing these interindividual variations in language network topography, MS-HBM enables reliable prediction of task-based language dominance. In this context, precision functional mapping provides a powerful approach to elucidate how chronic epileptogenic activity reorganizes resting-state cortical networks and influences cognitive function.<sup>44</sup> Importantly, we found that model performance plateaued at approximately 20–25 training participants, indicating that high-quality individual-specific networks can be achieved without requiring large training datasets. This is particularly encouraging for clinical populations where acquiring large-scale resting-state fMRI datasets may be challenging.

Future studies should validate the resting-state laterality index derived from MS-HBM against gold-standard measures, such as the intracarotid amobarbital test<sup>2</sup> or cortical electrical stimulation.<sup>45</sup> Although this study focused on language networks and their role in predicting language dominance, these results more broadly demonstrate that MS-HBM can reliably estimate individual-specific networks in patients with neurological disorders, even with limited resting-state fMRI data. This approach could be extended to predict other cognitive comorbidities<sup>42,46–49</sup> and postoperative functional

outcomes<sup>50–54</sup> in patients with drug-resistant epilepsy. Together, these findings suggest that MS-HBM may be applied to other clinical populations and neurological pathologies, offering a practical, noninvasive tool for presurgical evaluation and potentially guiding individualized clinical decision-making.<sup>55</sup>

Several limitations of our study should be acknowledged. The esfmri dataset provided a unique opportunity to validate individual-specific networks using evoked activity during concurrent intracranial electrical stimulation.<sup>27</sup> However, this dataset did not collect true postoperative resting-state fMRI, and we concatenated blocks of fMRI data when no stimulation was applied to simulate resting-state scans.<sup>33</sup> Comparisons of functional connectivity within the same participants across pre- and postoperative data revealed differences that may reflect (1) the effects of neurosurgery, (2) signal distortion due to implanted electrodes, or (3) scanner-related differences. Despite these factors, NIH MS-HBM consistently produced high-quality individual-specific networks across both pre- and postoperative data in the esfmri dataset. Finally, we studied participants with temporal lobe and extratemporal lobe epilepsy undergoing presurgical evaluation, and future studies are required to validate these networks in other types of drug-resistant epilepsy (e.g., idiopathic generalized epilepsy).

## 5 | CONCLUSIONS

In summary, we present a method for estimating reliable, high-quality, individual-specific cortical networks in drug-resistant epilepsy and show that individual-specific language network topography predicts task-based language dominance. Our model is publicly available ([https://github.com/ThomasYeoLab/CBIG/tree/master/stable\\_projects/brain\\_parcellation/Lim2026\\_MSHBM\\_epilepsy](https://github.com/ThomasYeoLab/CBIG/tree/master/stable_projects/brain_parcellation/Lim2026_MSHBM_epilepsy)), which may be used to estimate individual-specific cortical networks and predict language dominance in a new individual with drug-resistant epilepsy given at least 6 min of single-session resting-state fMRI data. In addition, a group-average parcellation derived from the combined NIH and esfmri drug-resistant epilepsy cohorts is made available as a resource for future studies (Figure S7).

### AUTHOR CONTRIBUTIONS

**Mervyn Jun Rui Lim:** Conceptualization; analysis and writing of the manuscript. **Shaoshi Zhang:** Conceptualization; supporting the analysis and reviewing of the manuscript. **Shreya Pande:** Supporting the analysis and reviewing of the manuscript. **Aihuiping Xue:** Supporting the analysis and reviewing of the manuscript.

**Ru Kong:** Supporting the analysis and reviewing of the manuscript. **Kareem Zaghloul:** Conceptualization; reviewing the analysis and manuscript. **Sara Inati:** Conceptualization; reviewing the analysis and manuscript. **B. T. Thomas Yeo:** Conceptualization; reviewing the analysis and manuscript.

### ACKNOWLEDGMENTS

None.

### FUNDING INFORMATION

Our research is supported by the NUS Yong Loo Lin School of Medicine (NUHSRO/2020/124/TMR/LOA), the Singapore National Medical Research Council (NMRC) LCG (OFLCG19May-0035), NMRC CTG-IIT (CTGIIT23jan-0001), NMRC OF-IRG (OFIRG24jan-0006; OFIRG24jul-0049), NMRC STaR (STaR20nov-0003), Singapore Ministry of Health (MOH) Center Grant (CG21APR1009), the US National Institutes of Health (R01MH133334 & 2R01MH120080), and the Singapore National Research Foundation Investigatorship (NRFI10-2024-0014). This study was also supported in part by NIH-DIR ZIA NS009431-05 from the Division of Intramural Research at the National Institute of Neurological Disorders and Stroke, US National Institutes of Health. Any opinions, findings, and conclusions or recommendations expressed in this material are those of the authors and do not reflect the views of the funders.

### CONFLICT OF INTEREST STATEMENT

The authors declare no conflicts of interest. We confirm that we have read the Journal's position on issues involved in ethical publication and affirm that this report is consistent with those guidelines.

### DATA AVAILABILITY STATEMENT

Deidentified data from the National Institutes of Health will be made available upon reasonable request to [sara.inati@nih.gov](mailto:sara.inati@nih.gov). All other data used are open source and available at their respective sites.

### ORCID

Mervyn Jun Rui Lim  <https://orcid.org/0000-0002-6866-9531>

Shaoshi Zhang  <https://orcid.org/0000-0002-6352-9150>


Shreya Pande  <https://orcid.org/0009-0009-5991-0969>

Aihuiping Xue  <https://orcid.org/0009-0008-7907-8594>

Ru Kong  <https://orcid.org/0000-0001-7842-0329>

Kareem Zaghloul  <https://orcid.org/0000-0001-8575-3578>

Sara Inati  <https://orcid.org/0000-0002-7587-5085>

B. T. Thomas Yeo  <https://orcid.org/0000-0002-0119-3276>

**REFERENCES**

1. Hermann BP, Wyler AR, Somes G, Clement L. Dysnomia after left anterior temporal lobectomy without functional mapping: frequency and correlates. *Neurosurgery*. 1994;35(1):52–7.
2. Binder JR, Swanson SJ, Hammeke TA, Morris GL, Mueller WM, Fischer M, et al. Determination of language dominance using functional MRI: a comparison with the Wada test. *Neurology*. 1996;46(4):978–84.
3. Lado FA, Ahrens SM, Riker E, Muh CR, Richardson RM, Gray J, et al. Guidelines for specialized epilepsy centers: executive summary of the report of the National Association of epilepsy centers guideline panel. *Neurology*. 2024;102(4):e208087.
4. Szaflarski JP, Gloss D, Binder JR, Gaillard WD, Golby AJ, Holland SK, et al. Practice guideline summary: use of fMRI in the presurgical evaluation of patients with epilepsy: report of the guideline development, dissemination, and implementation Subcommittee of the American Academy of neurology. *Neurology*. 2017;88(4):395–402.
5. Binder JR, Swanson SJ, Hammeke TA, Sabsevitz DS. A comparison of five fMRI protocols for mapping speech comprehension systems. *Epilepsia*. 2008;49(12):1980–97.
6. Gaillard WD, Berl MM, Moore EN, Ritzl EK, Rosenberger LR, Weinstein SL, et al. Atypical language in lesional and nonlesional complex partial epilepsy. *Neurology*. 2007;69(18):1761–71.
7. Fox MD, Greicius M. Clinical applications of resting state functional connectivity. *Front Syst Neurosci*. 2010;4:19.
8. Doucet GE, Pustina D, Skidmore C, Sharan A, Sperling MR, Tracy JI. Resting-state functional connectivity predicts the strength of hemispheric lateralization for language processing in temporal lobe epilepsy and normals. *Hum Brain Mapp*. 2015;36(1):288–303.
9. Phillips NL, Shatil AS, Go C, Robertson A, Widjaja E. Resting-state functional MRI for determining language lateralization in children with drug-resistant epilepsy. *AJNR Am J Neuroradiol*. 2021;42(7):1299–304.
10. Pur DR, Eagleson R, Lo M, Jurkiewicz MT, Andrade A, de Ribaupierre S. Presurgical brain mapping of the language network in pediatric patients with epilepsy using resting-state fMRI. *J Neurosurg Pediatr*. 2021;27(3):259–68.
11. Rolinski R, You X, Gonzalez-Castillo J, Norato G, Reynolds RC, Inati SK, et al. Language lateralization from task-based and resting state functional MRI in patients with epilepsy. *Hum Brain Mapp*. 2020;41(11):3133–46.
12. Bettus G, Guedj E, Joyeux F, Confort-Gouny S, Soulier E, Laguitton V, et al. Decreased basal fMRI functional connectivity in epileptogenic networks and contralateral compensatory mechanisms. *Hum Brain Mapp*. 2009;30(5):1580–91.
13. Ji GJ, Fox MD, Morton-Dutton M, Wang Y, Sun J, Hu P, et al. A generalized epilepsy network derived from brain abnormalities and deep brain stimulation. *Nat Commun*. 2025;16(1):2783.
14. Pittau F, Grova C, Moeller F, Dubeau F, Gotman J. Patterns of altered functional connectivity in mesial temporal lobe epilepsy. *Epilepsia*. 2012;53(6):1013–23.
15. Xie K, Sahlas E, Ngo A, Chen J, Arafat T, Royer J, et al. Personalized biomarkers of multiscale functional alterations in temporal lobe epilepsy. *Nat Commun*. 2025;16(1):10145.
16. Du J, DiNicola LM, Angeli PA, Saadon-Grosman N, Sun W, Kaiser S, et al. Organization of the human cerebral cortex estimated within individuals: networks, global topography, and function. *J Neurophysiol*. 2024;131(6):1014–82.
17. Gordon EM, Laumann TO, Adeyemo B, Petersen SE. Individual variability of the system-level Organization of the Human Brain. *Cereb Cortex*. 2017;27(1):386–99.
18. Gordon EM, Laumann TO, Gilmore AW, Newbold DJ, Greene DJ, Berg JJ, et al. Precision functional mapping of individual human brains. *Neuron*. 2017;95(4):791–807.
19. Laumann TO, Gordon EM, Adeyemo B, Snyder AZ, Joo SJ, Chen MY, et al. Functional system and areal Organization of a Highly Sampled Individual Human Brain. *Neuron*. 2015;87(3):657–70.
20. Laumann TO, Ortega M, Hoyt CR, Seider NA, Snyder AZ, Dosenbach NU, et al. Brain network reorganisation in an adolescent after bilateral perinatal strokes. *Lancet Neurol*. 2021;20(4):255–6.
21. Lynch CJ, Elbau IG, Ng T, Ayaz A, Zhu S, Wolk D, et al. Frontostriatal salience network expansion in individuals in depression. *Nature*. 2024;633(8030):624–33.
22. Filippi M, van den Heuvel MP, Fornito A, He Y, Hulshoff Pol HE, Agosta F, et al. Assessment of system dysfunction in the brain through MRI-based connectomics. *Lancet Neurol*. 2013;12(12):1189–99.
23. Kong R, Xue A, Ooi LQR, Asplund C, Tan XW, Goh SE, et al. Network-based near-scalp personalized Brain stimulation targets. 2025 bioRxiv, 2025.05.15.654391.
24. Roland JL, Smyth MD. Editorial. Mapping at rest: translating resting-state functional MRI to clinical practice. *J Neurosurg*. 2019;131(3):759–61.
25. Braga RM, Buckner RL. Parallel interdigitated distributed networks within the individual estimated by intrinsic functional connectivity. *Neuron*. 2017;95(2):457–71.
26. Kong R, Li J, Orban C, Sabuncu MR, Liu H, Schaefer A, et al. Spatial topography of individual-specific cortical networks predicts human cognition, personality, and emotion. *Cereb Cortex*. 2019;29(6):2533–51.
27. Thompson WH, Nair R, Oya H, Esteban O, Shine JM, Petkov CI, et al. A data resource from concurrent intracranial stimulation and functional MRI of the human brain. *Sci Data*. 2020;7(1):258.
28. Holmes AJ, Hollinshead MO, O’Keefe TM, Petrov VI, Fariello GR, Wald LL, et al. Brain genomics Superstruct project initial data release with structural, functional, and behavioral measures. *Sci Data*. 2015;2:150031.
29. Yeo BT, Krienen FM, Sepulcre J, Sabuncu MR, Lashkari D, Hollinshead M, et al. The organization of the human cerebral cortex estimated by intrinsic functional connectivity. *J Neurophysiol*. 2011;106(3):1125–65.
30. Lashkari D, Vul E, Kanwisher N, Golland P. Discovering structure in the space of fMRI selectivity profiles. *NeuroImage*. 2010;50(3):1085–98.
31. Gordon EM, Laumann TO, Adeyemo B, Huckins JF, Kelley WM, Petersen SE. Generation and evaluation of a cortical area Parcellation from resting-state correlations. *Cereb Cortex*. 2016;26(1):288–303.
32. Schaefer A, Kong R, Gordon EM, Laumann TO, Zuo XN, Holmes AJ, et al. Local-global Parcellation of the human cerebral cortex from intrinsic functional connectivity MRI. *Cereb Cortex*. 2018;28(9):3095–114.

33. Pedersen M, Zalesky A. Intracranial brain stimulation modulates fMRI-based network switching. *Neurobiol Dis.* 2021;156:105401.
34. Oya H, Howard MA, Magnotta VA, Kruger A, Griffiths TD, Lemieux L, et al. Mapping effective connectivity in the human brain with concurrent intracranial electrical stimulation and BOLD-fMRI. *J Neurosci Methods.* 2017;277:101–12.
35. Buckner RL, Krienen FM, Yeo BT. Opportunities and limitations of intrinsic functional connectivity MRI. *Nat Neurosci.* 2013;16(7):832–7.
36. Courtiol J, Guye M, Bartolomei F, Petkoski S, Jirsa VK. Dynamical mechanisms of Interictal resting-state functional connectivity in epilepsy. *J Neurosci.* 2020;40(29):5572–88.
37. van Diessen E, Zweiphenning WJ, Jansen FE, Stam CJ, Braun KP, Otte WM. Brain Network Organization in Focal Epilepsy: a systematic review and meta-analysis. *PLoS One.* 2014;9(12):e114606.
38. Caciagli L, Bernhardt BC, Hong SJ, Bernasconi A, Bernasconi N. Functional network alterations and their structural substrate in drug-resistant epilepsy. *Front Neurosci.* 2014;8:411.
39. Sisodiya SM, Whelan CD, Hatton SN, Huynh K, Altmann A, Ryten M, et al. The ENIGMA-epilepsy working group: mapping disease from large data sets. *Hum Brain Mapp.* 2020;43(1):113–28.
40. Bernhardt BC, Chen Z, He Y, Evans AC, Bernasconi N. Graph-theoretical analysis reveals disrupted small-world organization of cortical thickness correlation networks in temporal lobe epilepsy. *Cereb Cortex.* 2011;21(9):2147–57.
41. Liao W, Zhang Z, Pan Z, Mantini D, Ding J, Duan X, et al. Altered functional connectivity and small-world in mesial temporal lobe epilepsy. *PLoS One.* 2010;5(1):e8525.
42. Englot DJ, Konrad PE, Morgan VL. Regional and global connectivity disturbances in focal epilepsy, related neurocognitive sequelae, and potential mechanistic underpinnings. *Epilepsia.* 2016;57(10):1546–57.
43. van Diessen E, Diederer SJ, Braun KP, Jansen FE, Stam CJ. Functional and structural brain networks in epilepsy: what have we learned? *Epilepsia.* 2013;54(11):1855–65.
44. Robert S, Granovetter MC, Patterson C, Behrmann M. Hemispheric functional organization, as revealed by naturalistic neuroimaging, in pediatric epilepsy patients with cortical resections. *Proc Natl Acad Sci USA.* 2024;121(28):e2317458121.
45. Austermeuhle A, Cocjin J, Reynolds R, Agrawal S, Sepeta L, Gaillard WD, et al. Language functional MRI and direct cortical stimulation in epilepsy preoperative planning. *Ann Neurol.* 2017;81(4):526–37.
46. Ankeeta A, Zhang Q, Javidi SS, Modi S, Sperling MR, Tracy JI. Individualized functional and structural language Laterality in temporal lobe epilepsy and their impact on memory. *Hum Brain Mapp.* 2025;46(10):e70250.
47. Ren Z, Zhao Y, Han X, Yue M, Wang B, Zhao Z, et al. An objective model for diagnosing comorbid cognitive impairment in patients with epilepsy based on the clinical-EEG functional connectivity features. *Front Neurosci.* 2022;16:1060814.
48. Royer J, Larivière S, Rodriguez-Cruces R, Cabalo DG, Tavakol S, Auer H, et al. Cortical microstructural gradients capture memory network reorganization in temporal lobe epilepsy. *Brain.* 2023;146(9):3923–37.
49. Zhang Z, Zhou X, Liu J, Qin L, Yu L, Pang X, et al. Longitudinal assessment of resting-state fMRI in temporal lobe epilepsy: a two-year follow-up study. *Epilepsy Behav.* 2020;103:106858.
50. Akbarian B, Sainburg LE, Janson A, Johnson G, Doss DJ, Rogers BP, et al. Association between postsurgical functional connectivity and seizure outcome in patients with temporal lobe epilepsy. *Neurology.* 2024;103(7):e209816.
51. Bettus G, Bartolomei F, Confort-Gouny S, Guedj E, Chauvel P, Cozzone PJ, et al. Role of resting state functional connectivity MRI in presurgical investigation of mesial temporal lobe epilepsy. *J Neurol Neurosurg Psychiatry.* 2010;81(10):1147–54.
52. Boerwinkle VL, Cediél EG, Mirea L, Williams K, Kerrigan JF, Lam S, et al. Network-targeted approach and postoperative resting-state functional magnetic resonance imaging are associated with seizure outcome. *Ann Neurol.* 2019;86(3):344–56.
53. Boerwinkle VL, Mohanty D, Foldes ST, Guffey D, Minard CG, Vedantam A, et al. Correlating resting-state functional magnetic resonance imaging connectivity by independent component analysis-based epileptogenic zones with intracranial electroencephalogram localized seizure onset zones and surgical outcomes in prospective pediatric intractable epilepsy study. *Brain Connect.* 2017;7(7):424–42.
54. Wang F, Ren J, Cui W, Zhou Y, Yao P, Lai X, et al. Verbal memory network mapping in individual patients predicts postoperative functional impairments. *Hum Brain Mapp.* 2024;45(7):e26691.
55. Boerwinkle VL, Mirea L, Gaillard WD, Sussman BL, Larocque D, Bonnell A, et al. Resting-state functional MRI connectivity impact on epilepsy surgery plan and surgical candidacy: prospective clinical work. *J Neurosurg Pediatr.* 2020;25(6):574–81.

## SUPPORTING INFORMATION

Additional supporting information can be found online in the Supporting Information section at the end of this article.

**How to cite this article:** Lim MJR, Zhang S, Pande S, Xue A, Kong R, Zaghoul K, et al. Individual-specific resting-state networks predict language dominance in drug-resistant epilepsy. *Epilepsia.* 2026;00:1–13. <https://doi.org/10.1002/epi.70323>